

# Synapsin Condensates Recruit alpha-Synuclein

Christian Hoffmann <sup>1†</sup>, Roberto Sansevrino <sup>1†</sup>, Giuseppe Morabito <sup>1</sup>, Chinyere Logan <sup>1</sup>, R. Martin Vabulas <sup>2</sup>, Ayse Ulusoy <sup>3</sup>, Marcelo Ganzella <sup>4</sup> and Dragomir Milovanovic <sup>1\*</sup>

- 1 Laboratory of Molecular Neuroscience, German Center for Neurodegenerative Diseases (DZNE), 10117 Berlin, Germany
- 2 Charité Universitätsmedizin Berlin. Institute of Biochemistry, 10117 Berlin. Germany
- 3 Laboratory of Neuroprotective Mechanisms, German Center for Neurodegenerative Diseases (DZNE), 53127 Bonn, Germany
- 4 Department of Neurobiology, Max Planck Institute for Biophysical Chemistry, 37077 Göttingen, Germany

Correspondence to Dragomir Milovanovic: dragomir.milovanovic@dzne.de (D. Milovanovic) https://doi.org/10.1016/j.jmb.2021.166961

Edited by Richard W. Kriwacki

# **Abstract**

Neurotransmission relies on the tight spatial and temporal regulation of the synaptic vesicle (SV) cycle. Nerve terminals contain hundreds of SVs that form tight clusters. These clusters represent a distinct liquid phase in which one component of the phase are SVs and the other synapsin 1, a highly abundant synaptic protein. Another major family of disordered proteins at the presynapse includes synucleins, most notably  $\alpha$ -synuclein. The precise physiological role of  $\alpha$ -synuclein in synaptic physiology remains elusive, albeit its role has been implicated in nearly all steps of the SV cycle. To determine the effect of α-synuclein on the synapsin phase, we employ the reconstitution approach using natively purified SVs from rat brains and the heterologous cell system to generate synapsin condensates. We demonstrate that synapsin condensates recruit  $\alpha$ -synuclein, and while enriched into these synapsin condensates,  $\alpha$ -synuclein still maintains its high mobility. The presence of SVs enhances the rate of synapsin/α-synuclein condensation, suggesting that SVs act as catalyzers for the formation of synapsin condensates. Notably, at physiological salt and protein concentrations, α-synuclein alone is not able to cluster isolated SVs. Excess of α-synuclein disrupts the kinetics of synapsin/SV condensate formation, indicating that the molar ratio between synapsin and α-synuclein is important in assembling the functional condensates of SVs. Understanding the molecular mechanism of α-synuclein interactions at the nerve terminals is crucial for clarifying the pathogenesis of synucleinopathies, where  $\alpha$ -synuclein, synaptic proteins and lipid organelles all accumulate as insoluble intracellular inclusions.

© 2021 The Author(s). Published by Elsevier Ltd. This is an open access article under the CC BY license (http://creativecommons.org/licenses/by/4.0/).

# Introduction

Neuronal communication depends on the tightly regulated spatial and temporal release of the messenger molecules known as neurotransmitters. Neurotransmitters are packed into synaptic vesicles (SVs) and nerve terminals contain hundreds of SVs that are tightly clustered. Despite

being held together in these clusters, SVs are highly mobile. This allows them to be swiftly recruited to the neuronal plasma membrane to release their content upon activation of the neuron.<sup>2,3</sup>

Several features of SV clusters suggest that they have fluid-like properties. For example, SV clusters have homogeneous structures with sharp boundaries and exclude other organelles despite the

absence of a specific barrier that delimits them.<sup>1,5</sup> While being tightly clustered, SVs appear to be mobile both within the clusters and between the cluster and the surrounding cytoplasm.<sup>6</sup> It was proposed that liquid–liquid phase separation could underlie this compact clustering of SVs while maintaining their high mobility.<sup>4</sup> Indeed, reconstitution studies showed that synapsin 1, the major synaptic phosphoprotein,<sup>7,8</sup> can form liquid condensates that actively sequester lipid vesicles via its long intrinsically disordered region (IDR).<sup>9</sup> Phosphorylation of Synapsin IDR by CaMKII disperses synapsin condensates,<sup>9</sup> mimicking the dispersion of SVs observed in living synapses.<sup>10</sup>

Apart from Synapsins, another protein family that lacks a stable tertiary structure, is the family of Synucleins ( $\alpha$ -,  $\beta$ -, and  $\gamma$ -synuclein). In the past three decades,  $\alpha$ -synuclein has been under the spotlight because of its involvement in neurodegenerative diseases, collectively called synucleinopathies, not the least Parkinson's disease (PD).  $\alpha$ -Synuclein is highly abundant at the nerve terminal. It is structurally unfolded in solution and in cells  $\alpha$ - or it forms transient tetramers.  $\alpha$ - Upon binding to negatively charged membranes, the N-terminal domain of  $\alpha$ -synuclein folds into an  $\alpha$ -helix  $\alpha$ - and was shown to form oligomers at the surface of SVs.

The precise physiological role of  $\alpha$ -synuclein in synaptic physiology remains elusive, albeit its role has been implicated in nearly all steps of SV cycle.<sup>21–24</sup> A recent analysis of neurons in culture showed that overexpression of α-synuclein attenuates neurotransmitter release but only in the presence of synapsin, suggesting a functional interaction between the two proteins.<sup>25</sup> Interestingly, while genetic deletion of three synapsin genes results in dispersion of SVs from the nerve terminals in mice both in culture <sup>26,27</sup> and *in situ*, <sup>9</sup> the analyses of nerve terminals in mice that lack all three synucleins showed, different from the wild type situation, a nearly crystalline-packing of SVs. 28 Given that these synuclein triple-KO mice still expressed synapsin,<sup>28</sup> the presence of SV clusters is not surprising, but the tight liquid-crystalline architecture of these clusters suggests a fundamental alteration of its material properties. The interaction between synapsin and α-synuclein has been mostly established in overexpressed conditions, 25,29 so the precise mechanism that underlies their association under physiological conditions, either direct or indirect. remains elusive.

Here, we employ the heterologous cell system to ectopically generate synapsin condensates and reconstitution approaches using natively purified SVs isolated from rat brains to determine the effect of  $\alpha$ -synuclein recruitment in the synapsin condensates. We show that, at physiological concentrations and salt conditions,  $\alpha$ -synuclein alone is not able to cluster native SV. However,  $\alpha$ -synuclein is enriched into synapsin condensates,

while still maintaining its high mobility. Interestingly, excess of  $\alpha$ -synuclein disrupts the kinetics of synapsin/SV condensate formation, indicating that the molar ratio between synapsin and  $\alpha$ -synuclein is important in assembling the functional condensates of SVs.

## Results

For imaging in cells, we tagged human synapsin 1 and  $\alpha$ -synuclein with mCherry and blue fluorescent protein (BFP), respectively. Given that synapsin 1 has a long intrinsically disordered domain at the C-terminus (8 and Figure S1), the tag was cloned at its N-terminus. For  $\alpha$ -synuclein, a protein that is nearly entirely disordered in solution (15,16, Figure S1), we fused BFP to its C-terminus since this construct maintains its N-terminal ability to SVs as shown for the untagged protein. Overexpressed in primary hippocampal neurons, both mCherry-synapsin 1 and  $\alpha$ -synuclein-BFP localize to synaptic boutons (Figure 1(a), Figure S1).

Ectopic overexpression of either mCherrysynapsin 1 (Figure 1(b), Figure S2) or α-synuclein-BFP (Figure 1(c), Figure S2) alone in a nonneuronal cell line such as a HEK cells results in a diffuse signal in the cytosolic region suggesting soluble proteins. On some occasions, small puncta can be noticed close to the plasma probably reflecting membrane. synapsin interaction with actin.31 However, co-expression of mCherry-synapsin 1 and α-synuclein-BFP results in the appearance of large fluorescent foci enriched with both proteins (Figure 1(d), Figure S2). The appearance of these droplets was dependent on the amount of transfected plasmid (Figure S2). Purifying recombinant mCherry and imaging a dilution series of known concentrations under the same laser power as we performed the live-cell imaging, suggests that 1 µM is the total cell concentration of mCherry-synapsin 1 above which we start seeing droplets. Condensates of mCherry-synapsin 1 and α-synuclein-BFP are distinct from puncta formed by overexpression of FUS-EGFP, an RNA-binding protein known to phase separate (Figure S3).

To examine whether condensates of mCherrysynapsin 1 and α-synuclein-BFP are dynamic, we turned to fluorescence recovery photobleaching (FRAP) measurements. Indeed, bleaching both mCherry-synapsin 1 and  $\alpha$ synuclein-BFP condensates results recovery of fluorescence (Figure 2(a)) indicating their fluid nature. While for  $\alpha$ -synuclein-BFP the entire fluorescence signal recovered both within a condensate and in soluble pool, for mCherrysynapsin 1, only about 40% of total fluorescence within a condensate recovered. This suggests mCherry-synapsin 1 acting as a scaffold molecule building a condensate and α-synuclein-BFP being transiently enriched in these condensates.

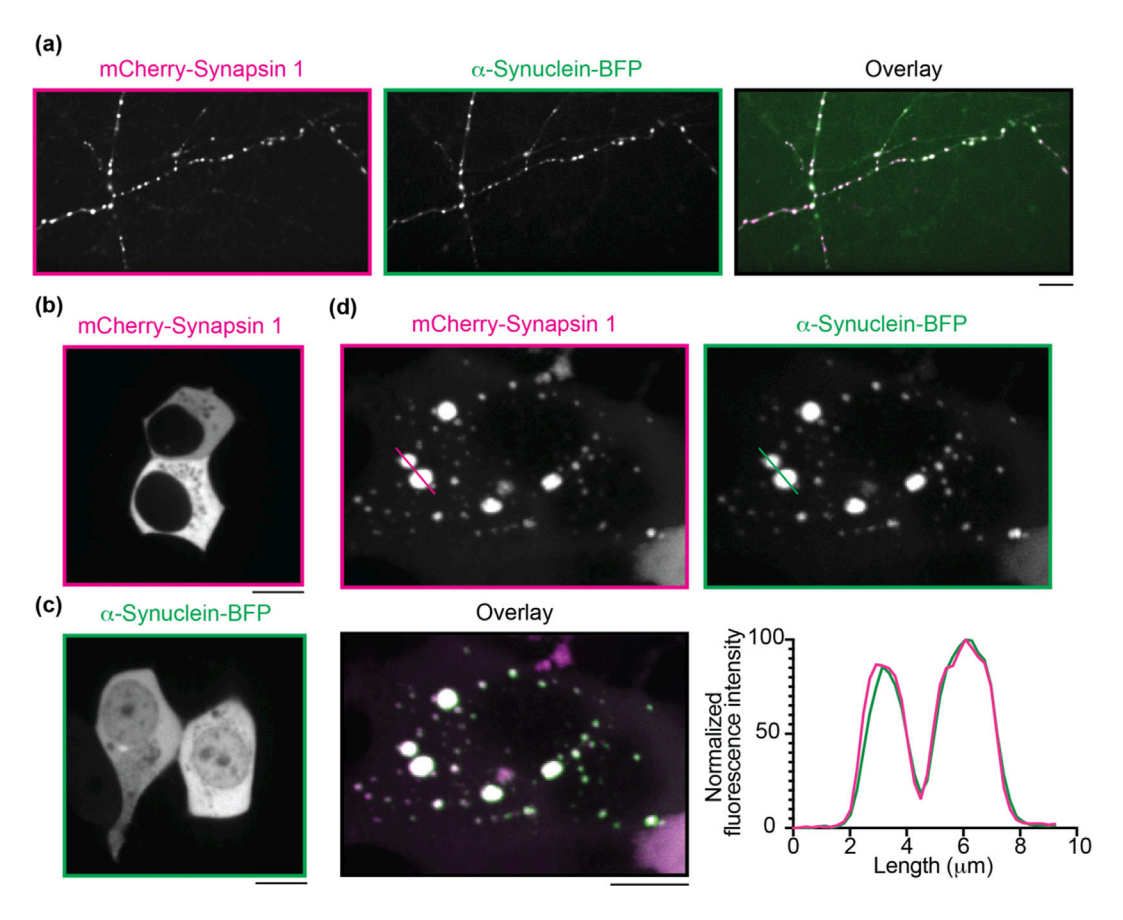


Figure 1. Interaction of synapsin 1 and  $\alpha$ -synuclein in cells. (a) Both mCherry-synapsin 1 and  $\alpha$ -synuclein-BFP constructs are targeted to synapses in primary hippocampal neurons. Heterologous expression of mCherry-Synapsin 1 (b) and  $\alpha$ -synuclein-BFP (c) in HEK293T cells results in mostly diffuse distribution. (d) Co-expression of both mCherry-synapsin 1 and  $\alpha$ -synuclein-BFP results the formation of condensates. Line profiles indicate that both proteins co-localize in puncta. Scale bars, 10 µm.

Another suitable assay to distinguish fluid condensates from insoluble aggregates is to measure the effect of the aliphatic alcohol 1,6hexanediol on condensates. If fluid, condensates will be dissolved by the addition of 1,6hexanediol. 32,33 Indeed, condensates of mCherrysynapsin 1 and  $\alpha$ -synuclein-BFP disperse after adding of the final concentration 3% 1,6-hexanediol (Figure 3). This effect is specific to 1,6-hexanediol since shorter aliphatic alcohol, 1,3-propanediol, has a lower potency for dissolving the condensates (Figure S4). That mCherry-synapsin 1 and  $\alpha$ synuclein-BFP coexpressed in cells form droplets. might be due to overall high concentrations. local crowding in cells, and phosphorylation state of proteins.

After characterizing the condensates that arise by ectopic co-expression of mCherry-synapsin 1 and  $\alpha$ -synuclein-BFP, we turned to minimal reconstitution system using recombinant proteins, liposomes and natively purified synaptic vesicles (SVs) (Figure S5). For assay readout, we used turbidity measurements for quantifying the rate of condensate formation similarly as in 9. Here, the

formation of condensates and the increase of molecular packing results in the increase of turbidity at 405 nm. Synapsin 1 (6 µM) is known to form condensates<sup>9</sup> and the presence of molecular crowder – in our case 3% PEG 8000 – speeds up the reaction (Figure 4(a), magenta dashed curve).  $\alpha$ -Synuclein (2 μM), on the other hand, fails to undergo phase separation even in the presence of 3% PEG 8000 (Figure 4(a), green full and green dashed curves). The condition in which  $\alpha$ -synuclein is added to synapsin 1 at the physiological molar ratio 3:1 (synapsin 1-to- $\alpha$ -synuclein)<sup>13</sup> has the same kinetics of condensation as synapsin 1 alone (Figure 4(a), blue curve). Importantly, at the conditions used (concentrations, crowding and duration of assay, salt concentration),  $\alpha$ -synuclein is not forming fibrils (Figure 4(b)).

We further reconstituted EGFP-Synapsin 1 and  $\alpha$ -synuclein chemically labeled with far-red dye (Alexa Fluor 647) for microscopy visualization. Indeed, droplets of EGFP-Synapsin 1 at 3% PEG 8000 and physiological salt concentration (150 mM NaCl) recruit  $\alpha$ -synuclein (Figure 4(c)). Bleaching of either EGFP-Synapsin 1 or  $\alpha$ -

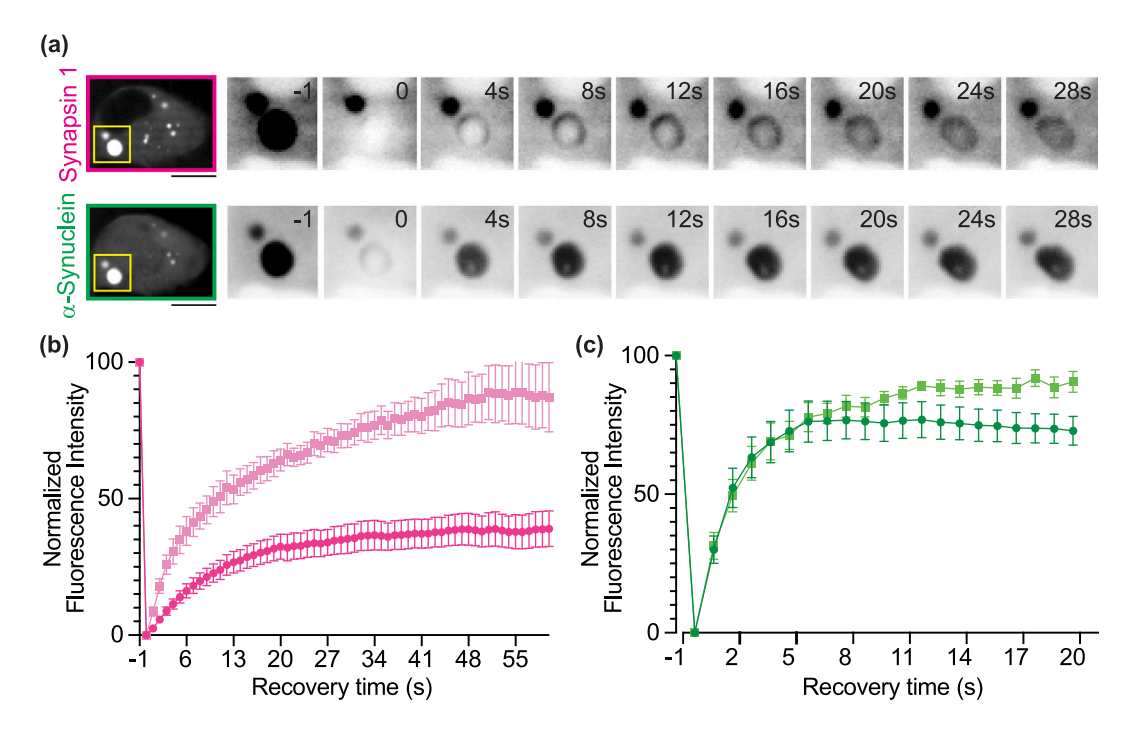


Figure 2. α-Synuclein retains its mobility in synapsin condensates. (a) FRAP of mCherry-synapsin 1 (top) and α-synuclein-BFP (bottom) in a droplet (highlighted in yellow). (b) Recovery after bleaching of mCherry-synapsin 1 in droplets (dark magenta) and in cytosol (light magenta). (c) Recovery after bleaching of α-synuclein-BFP in droplets (dark green) and in cytosol (light green). Values are represented as average  $\pm$  standard error of the mean. Data are from three independent biological replicates (ten cells each). Scale bars, 10 μm.

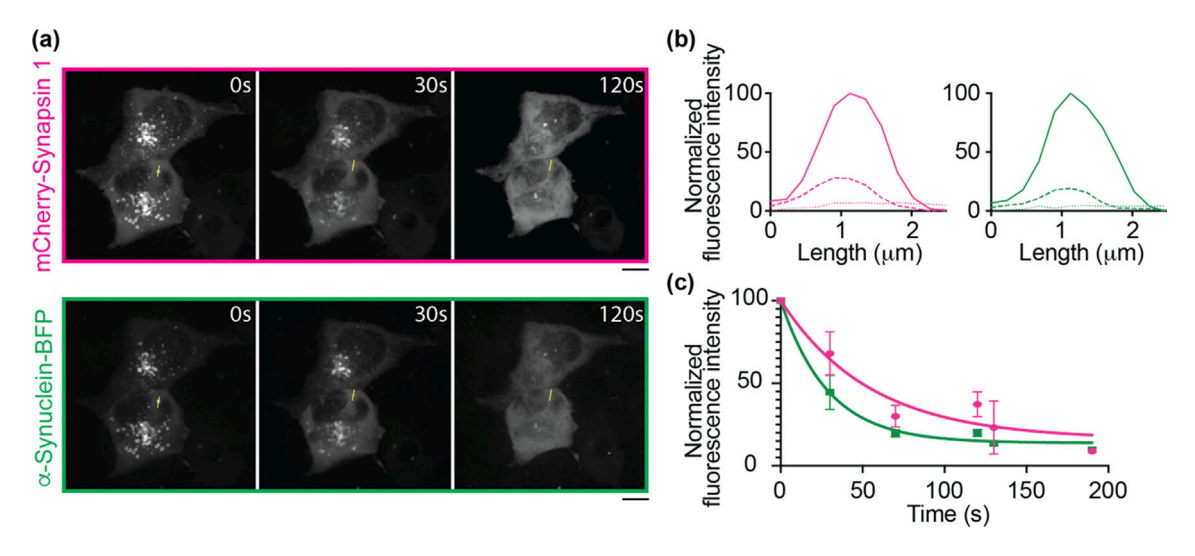


Figure 3. 1,6-Hexanediol disperses synapsin  $1/\alpha$ -synuclein condensates. (a) Confocal images of mCherry-synapsin 1 (top) and  $\alpha$ -synuclein-BFP (bottom) before (0 s) and after loading 3% 1,6-hexanediol (final concentration). Scale bars, 10  $\mu$ m. (b) Line profiles of mCherry-synapsin 1 (left) and  $\alpha$ -synuclein-BFP (right) for different time points (full line - 0 s, dashed line - 30 s, dotted line - 120 s). (c) Dispersion profiles of both mCherry-synapsin 1 and  $\alpha$ -synuclein-BFP from four independent experiments.

synuclein is followed by the recovery of fluorescence signal, indicating fluid nature of these condensates (Figure 4(d)). Similarly to FRAP experiments in cells,  $\alpha$ -synuclein shows full recovery unlike EGFP-Synapsin 1 where a large

immobile fraction is observed. This strongly indicates that  $\alpha$ -synuclein is transiently recruited to synapsin droplets.

To assess the contribution of SVs to condensation of synapsin 1 and  $\alpha$ -synuclein, we

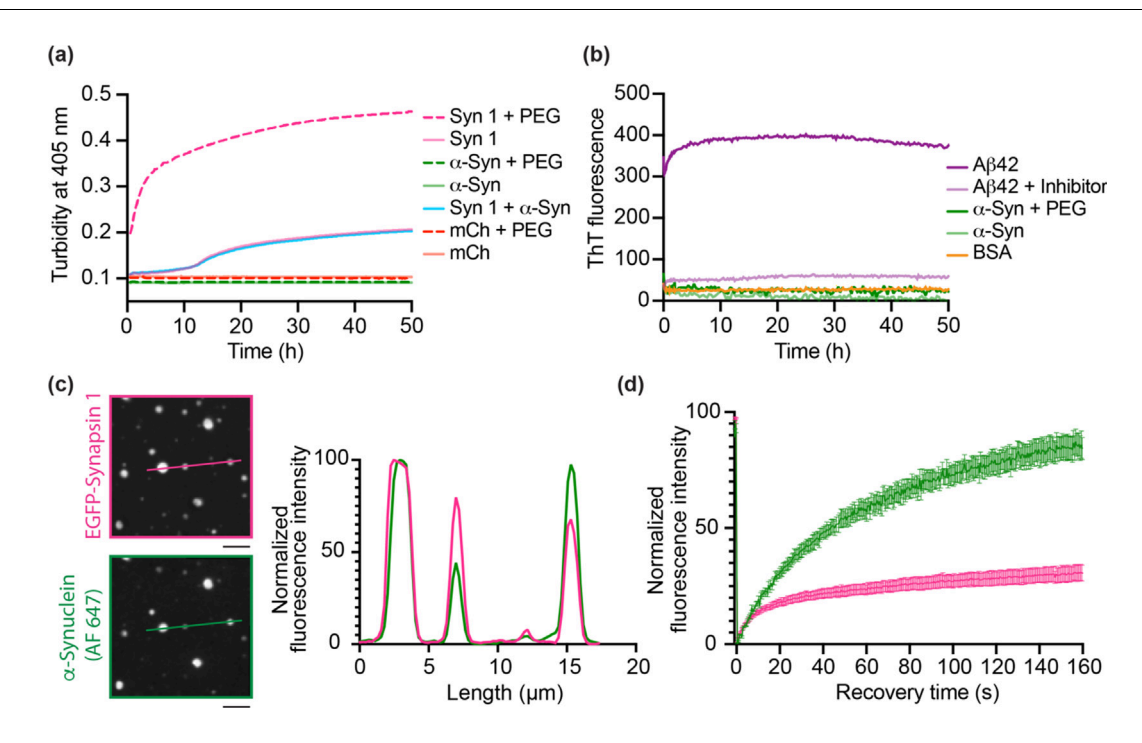


Figure 4. Condensate formation of purified recombinant proteins. (a) 6 μM EGFP-synapsin 1 in magenta; 6 μM mCherry in red; 2 μM  $\alpha$ -synuclein in green in the absence (full line) or presence of 3% PEG 8000 (dashed line). The condensate formation was measured as a change in turbidity at 405 nm. (b) Thioflavin T-based aggregation assay of 2 μM  $\alpha$ -synuclein (light green), 40 μM  $\alpha$ -synuclein in 15% PEG 8000 (dark green), 46 μM amyloid- $\beta$  1–42 (positive control, dark purple), 46 μM amyloid- $\beta$  1–42 with inhibitor compound (negative control, light purple), and 46 μM BSA (orange). (c) Colocalization of reconstituted condensates containing EGFP-Synapsin 1 (6 μM) and  $\alpha$ -synuclein (2 μM, chemically labeled with Alexa Fluor 647, AF 647) in 3% PEG, 8000. Scale bars, 5 μm. (d) Recovery after bleaching of  $\alpha$ -synuclein (AF 647) (green) and EGFP-Synapsin 1 (magenta). Values are represented as average  $\pm$  standard error of the mean. Data are from three independent reconstitutions.

chose the condition at which synapsin is not phase separating, which is 3  $\mu$ M synapsin without any crowding reagent, and supplemented it with physiological ratio of  $\alpha$ -synuclein (3:1). At this condition optical density remains unchanged (Figure 5). However, co-incubating the protein mixture with increasing amounts of native SVs (5.9 nM, 11.5 nM, 23 nM, 35 nM and 70 nM) purified from rats triggered the condensation (Figure 5). In fact, we observed that raising the amounts of SVs increases the extent of condensation. Despite its ability to cluster small liposomes and SVs,  $^{39-42}$   $\alpha$ -synuclein alone was not sufficient to form condensates with SVs at physiological molar ratios and salt concentrations (Figure 6, green curve).

The average synapsin to SV ratio is projected to be between 1:100 and 1:1000, and the ratio of synapsin to  $\alpha$ -synuclein is projected to be 3:1<sup>13</sup> prompting us to explore the significance of maintaining this molar relationship. Here, we coincubated synapsin and  $\alpha$ -synuclein in three different ratios (1:1, 1:3, and 3:1) while maintaining the concentration of SVs constant. In conditions where synapsin was present at a higher or equimolar ratio to  $\alpha$ -synuclein (Figure 6(a), dark and light blue

curves, respectively), the rate of condensation was nearly the same as when synapsin 1 was coincubated alone with SVs (Figure 6(a), magenta curve). However, the molar excess of  $\alpha$ -synuclein over synapsin 1 (Figure 6(a), turquoise curve) decreases the rate of synapsin-mediated condensate formation. In a complementary assay, the concentration of synapsin 1 was fixed at 2  $\mu$ M and  $\alpha$ synuclein was added to reach either 3:1 or 1:3 molar ratio (Figure S6). Here, data indicate that, at low concentrations of α-synuclein, the synapsin/SV condensation follows sigmoidal kinetics and, at higher concentrations of  $\alpha$ -synuclein, the condensation is steady without an apparent saturation plateau. Together, this implies the relevance of maintaining the tight balance of molar ratios between synapsin and α-synuclein for SV packing at the nerve terminals (Figure 6(b)).

# **Discussion**

Four main conclusions can be drawn from our data. First, synapsin condensates recruit  $\alpha$ -synuclein. Moreover,  $\alpha$ -synuclein maintains its high mobility within synapsin condensates. This

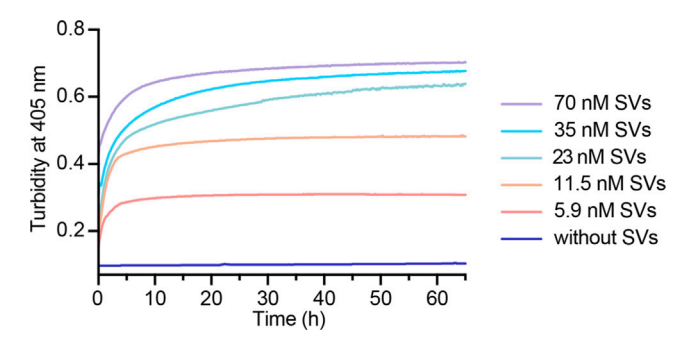


Figure 5. Synaptic vesicles promote the formation of synapsin condensates. Reconstitution of  $\alpha$ -synuclein (1  $\mu$ M) and EGFP-synapsin 1 (3  $\mu$ M), with increasing concentrations of SVs. The kinetics of condensate formation, assessed as a change in turbidity, increases with the increase of SV concentration.

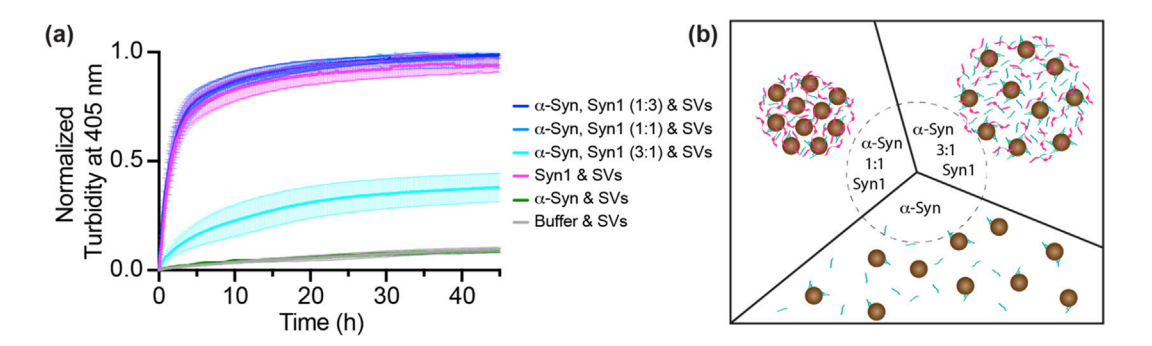


Figure 6. Excess of α-synuclein reduces the rate of synapsin condensate formation. (a) Condensate formation of purified recombinant proteins EGFP-synapsin 1 and α-synuclein in different molar ratios (curves in tones of blue), EGFP-synapsin 1 alone (magenta), α-synuclein alone (green) in presence of 23 nM SVs. The condensate formation was measured as a change in turbidity at 405 nm. Each value is shown as the average  $\pm$  standard error of the mean, data are from three independent replicates (each time fresh isolation of native SVs). (b) Scheme of the synapsin/SV condensation in the presence of different molar ratios of α-synuclein (α-synuclein-to-synapsin, 1:1 left and 3:1 right) or in the absence of synapsin (bottom).

implies that synapsin/SV condensates at the nerve terminals are able to spatially enrich  $\alpha\text{-synuclein},$  in line with SV clusters acting as a buffer of synaptic proteins.  $^{34-36}$  In fact, the dispersion of synapsin/vesicle condensates upon stimulation  $^{10}$  releases transiently-enriched proteins such as  $\alpha\text{-synuclein},$  which can subsequently translocate to the plasma membrane and facilitate endocytosis and SV recycling.  $^{23,37}$ 

Second, SVs act as triggers for the phase separation of synapsin. The presence of SVs enhances the rate of synapsin/ $\alpha$ -synuclein condensation (Figure 5). Titration of SVs into synapsin/ $\alpha$ -synuclein condensates fits well a linear curve. In this empirical model, the slope represents the number of protein molecules directly bound to SVs, which matches well previous quantitative assessments. Beyond enhancing the rate of condensate formation,  $\alpha$ -synuclein, at the surface of SVs, forms oligomers, helps assemble the SNARE complexes, thereby stimulating exocytosis. This while only a fraction of  $\alpha$ -synuclein might be enriched in SV clusters, the dynamic distribution of  $\alpha$ -synuclein – even a compe-

tition – for binding to different protein and membrane structures present at the presynapse remains to be understood. This is particularly important given the roles of  $\alpha$ -synuclein in mitochondria physiology, endocytic processes, or to stabilize SNARE complexes.  $^{21-24}$ 

Third,  $\alpha$ -synuclein alone, under physiological salt concentrations, cannot induce phase separation of native SV purified from rat brains (Figure 6). Although  $\alpha$ -synuclein binds to small, acidic lipid vesicles and SVs, 30,43,44 our results clearly show that, at physiological concentrations,  $\alpha$ -synuclein alone does not result in liquid–liquid phase separation of native SVs. However, at these protein and salt concentrations, vesicles enhance the rate of synapsin/ $\alpha$ -synuclein condensate formation.

Fourth, the excess molar ratio of  $\alpha$ -synuclein slows down the rate of synapsin/SV condensate formation. In situ analyses of nerve terminals in mice that lack all three synucleins showed, different from the wild type situation, a nearly crystalline-packing of SVs. <sup>28</sup> Given that synuclein TKO mice have smaller buttons <sup>22</sup> and still express

synapsin, which is essential and sufficient for SV cluster formation,  $^{45}$  the presence of tight SV clusters is not surprising. However, the liquid-crystalline arrangement of SVs $^{28}$  suggests an alteration of its material properties. Our reconstitution data now show that an excess of  $\alpha$ -synuclein slows down the rate of native SV condensation (Figure 6), implying that a tight balance between synapsin 1 and  $\alpha$ -synuclein is important for maintaining the architecture of SV clusters.

α-Synuclein aggregates appear in the range of disorders collectively referred synucleinopathies.46 From a pathological standpoint, a-synuclein accumulates predominantly at the presynaptic terminals in patient brains affected with synucleinopathies causing changes in synaptic function and leading to neurodegeneration.<sup>47</sup> It is therefore crucial to understand the functional implications of the regulation of α-synuclein abundance at the synapse. Functionally, the excess amounts of  $\alpha$ -synuclein in wild-type murine synapses results in a decrease of SV release and recycling. 48 Interestingly, this phenotype is absent when  $\alpha$ synuclein is overexpressed in neurons derived from synapsin TKO animals<sup>25</sup> indicating a functional interplay between these proteins. Since our data suggest that α-synuclein and synapsin associate as biomolecular condensates, it is tempting to speculate that multivalent low-affinity interactions would play an important role in their condensation. 49 One such candidate is synaptobrevin 2, an integral protein of SVs that interacts with α-synuclein. While  $\alpha$ -synuclein and synaptobrevin 2 might increase clustering of SVs, 42 they are not sufficient to induce mesoscale condensation of native SVs (Figure 5). On the other hand, acidity of SVs seems to play an important role in synapsin/lipid vesicle condensation (Figure S5 and Ref. 9) as neutral liposomes have no effect on enhancing condensation. The affinity of  $\alpha$ -synuclein for negatively charged phospholipids might be of critical importance<sup>5</sup> to locally enrich α-synuclein into synapsin/SV condensates.

The liquid-liquid phase separation might be on a reaction trajectory to aggregation of α-synuclein similarly to aggregates formed by RNA-binding proteins in other neuroand musculardegenerative diseases. 53,54 In fact, at pathologically high concentrations (e.g., 200 μM in 10% PEG 8000),  $\alpha$ -synuclein is able to form liquid condensates en route to aggregation. 55 These aggregates disrupt both the SV cycle<sup>48</sup> and mitochondrial physiology. Recent data suggest that α-synuclein aggregates are more complex than it was previously thought and may be composed not only of  $\alpha$ -synuclein and other proteins, but also by disrupted intercellular membranes and organelle remnants.5

In conclusion, we show that synapsin condensates are able to sequester  $\alpha$ -synuclein, both by co-expression with of  $\alpha$ -synuclein in heterologous cells and in minimal reconstituted

system with native SVs under physiological ion strength and protein concentrations. Our study emphasizes the importance of the molar ratio of synapsin and of  $\alpha$ -synuclein in the kinetics of condensate formation. It is important to reiterate that liquid–liquid phase transitions depend on the valency, affinity and concentrations. <sup>49,54</sup> In that context, our work opens a range of important questions such as what the precise molecular mechanism underlies the low-affinity association between synapsin and  $\alpha$ -synuclein; how this association is regulated during depolarization; and what the effect is of numerous other synaptic proteins enriched at the SV cluster.

### **Materials and Methods**

# Cloning

Synapsin 1 open reading frame was inserted into the pmCherry-C1 or pEGFP-C1 vector using BgIII-SacI restriction sites (Genscript). pEGFP-C1 and pmCherry-C1 were modified through NheI-XhoI sites to encode the His6-tag, according to 9  $\alpha$ -Synuclein (Addgene #51437) was PCR-based cloned using restriction sites BamHI-XhoI sites into a BFP-containing vector (kind gift from Geert van den Bogaart) to obtain C-terminally tagged  $\alpha$ -synuclein-BFP. All the vectors contain CMV promoter and SV40 terminator. Synaptophysin-EGFP (kind gift of Pietro De Camilli) and FUS-EGFP plasmid (kind gift of Susanne Wegmann) were both in pEGFP-N1 vector.

#### Cell culture and transfection

HEK cells were maintained at 37 °C and 5% CO<sub>2</sub> in Dulbecco's Modified Eagle's Medium (DMEM, Gibco) supplemented with 10% FBS (FACS), 1% Glutamax (Gibco), 1% non-essential amino acids (Sigma Aldrich) and 0.5% penicillin/streptomycin (Gibco). Cells were split every 2–3 days using 0.05% trypsin (Gibco).

Hippocampal neurons were prepared from P0 wild-type mice (C57BL6/J). Brains were manually dissected and hippocampi were collected in cold Hank's balanced salt solution (HBSS, Gibco) containing 10 mM Hepes buffer (Gibco), 1 mM Pyruvic Acid (Gibco), 0.5% penicyllin/streptomycin and 5.8 mM Magnesium Chloride. dissection. hippocampi were enzymatically digested with Papaine (Sigma) in HBSS for 20 min at 37 °C. Papaine was removed with repeated HBSS washing, and plating medium was added (Neurobasal Medium Α [NB-A, Gibco], supplemented with 5% FBS, 1% B27, 1x Glutamax, and 1% penicillin/streptomycin). Final cell suspension was obtained through mechanical dissociation with a P1000 pipette. Cells were seeded on glass coverslips coated with 0.1 mg/mL (PLL; Sigma). Neurons poly-L-lysine

maintained at 37 °C and 5% CO<sub>2</sub> in Neuronal Media (NB-A supplemented with 1% B27, 1% Glutamax, and 0.5% penicillin/streptomycin).

Cells were transfected by Lipofectamine 2000 following (Thermo Fisher) manufacturer's instructions. Briefly, 3 µl of lipofectamine 2000 was mixed with  $2 \mu g$  of total DNA in 200  $\mu l$ OptiMEM (Gibco) for HEK cells or NB-A for neurons. Transfection mix was incubated for 30 minutes at room temperature, then was added to the cells. HEK cells were transfected and incubated overnight (37 °C and 5% CO2). The day after medium was fully replaced with fresh supplemented DMEM. Neurons were transfected after 12 days in culture and incubated at 37 °C and 5% CO2. After 2 hours, medium was changed with Neuronal Medium.

All animal experiments were approved by the Institutional Animal Welfare Committees of the Charité University Clinic (Berlin, DE) and Max Planck Institute for Biophysical Chemistry (Göttingen, DE).

# Confocal fluorescence live-cell microscopy

Spinning disk confocal (SDC) microscopy was carried out on an Eclipse Ti Nikon Spinning Disk Confocal CSU-X, equipped with OkoLab Live-cells incubator (for control of temperature at 37 °C, 5% CO<sub>2</sub>), 2 EM-CCD cameras (AndorR iXon 888-U3 ultra EM-CCD), Andor Revolution SD System (CSU-X), objectives PL APO 60×/1.4NA oil immersion lens. Excitation wavelengths were: 405-nm for BFP, 488-nm for EGFP; 561-nm for mCherry.

For imaging, one or more constructs were transfected in HEK 293 cells or primary hippocampal neurons using Lipofectamine 2000 (Thermo Fisher). During imaging, cells seeded on glass coverslips (1.5 thickness, 25 mm diameter) were placed in a microscopy adaptor and then placed on the objective stage. Exposure time 200 ms, Gain 300 (EM gain 20 mHz 16-bit) and Piezo stage z-motor was used to collect z-series. Images were acquired using Acquisition software NIS Elements 5.21.02 and then analyzed with ImageJ (NIH).

1,6-Hexanediol assay. 1,6-Hexanediol (Sigma) was dissolved in DMEM (0,3 g/mL stock solution). HEK cells expressing  $\alpha\text{-Synuclein-BFP}$  and mCherry-Synapsin 1 were added a pre-warmed 1,6-hexanediol solution diluted to final concentration of 3% in DMEM (culture media) and imaged for various times as indicated in the text. All images were analyzed with ImageJ (NIH).

FRAP experiments and data analysis. Fluorescence recovery after photobleaching (FRAP) experiments were performed in HEK 293 cells expressing  $\alpha$ -Synuclein-BFP and mCherry-Synapsin1. The bleach ROI was fixed to 1.12  $\mu$ m

of diameter and bleached at 100% transmission intensity (405 nm = 3.5 mW and 561 nm = 4.1mW) for 500 ms. Recording were carried out starting with 1 picture pre-bleach, followed by bleach event and a post-bleach time-laps images were collected (1 s frame rate) up to 180 s. Reference ROI were defined in the cytosol of the same cell, and the Background ROI were defined outside of the cell. Each FRAP experiment was performed in at least 3 independent biological replications (different transfections). Intensity recovery traces obtained from the regions of interest were background corrected and all traces were normalized. The average trace was fitted to a simple linear regression function (Prism 9, Graphpad) obtaining the half time of recovery. All data are presented as mean ± s.e.m.

# Confocal imaging and FRAP of reconstituted condensates

Chemical labeling of a-synuclein. For chemical labeling of  $\alpha$ -synuclein the NHS-ester reactive fluorescent Alexa 647 dye from Thermo Scientific was used (Alexa647-NHS-Ester, 10 mg/ml). Labeling was performed in PBS (pH 8,3 with NaHCO<sub>3</sub>) for 1 h at room temperature with a 10 times molar excess of NHS-ester dye. Notconjugated dye was removed from labeled αsynuclein by running the labeling reaction over a column PD-10 and elution with PBS (Sephadex™G-25 M, GE Healthcare).

*Microscopy.* A mixture of 6 μM EGFP-Synapsin 1 was mixed with 2  $\mu$ M  $\alpha$ -synuclein (equimolar amounts of unlabeled and Alexa Fluor 647-labled) was incubated with in 25 mM Tris-HCI (pH 7.4), 150 mM NaCl, 0.5 mM TCEP. After the addition of 8000 (final concentration), PEG condensation reaction was transferred to a Glass Bottom Slide (81507, Ibidi) for imaging. The ROI was fixed to approx. 1.5 µm diameter and bleached 100% transmission at intensity (488 nm = 3.9 mW, 640 nm = 4.7 mW) for500 ms. Recording was carried out starting with a prebleach sequence, followed by the bleach event and post-bleach images were acquired up to 160 s (250 ms frame rate). Intensity recovery traces obtained from the regions of interest were background corrected and all traces were normalized. All data are presented as mean ± s.e.m.

## Protein expression and purification

EGFP-Synapsin 1 and mCherry were expressed in Expi293F™ cells (Thermo Fisher Scientific) for three days following enhancement. Cells were harvested and lysed in buffer that contained 25 mM Tris–HCl (pH 7.4), 300 mM NaCl, 0.5 mM TCEP (buffer A), and protease inhibitor (Complete

EDTA-free, Roche). All purification steps were carried out at 4 °C. The lysates were centrifuged for 1 h at 20,000*g*, followed by a two-step purification. The first step was affinity purification on a Ni-NTA column (HisTrap™HP, GE Healthcare) using 25 mM imidazole for binding of proteins, 40 mM during wash steps and 400 mM imidazole for elution of proteins (all in buffer A). Eluates were concentrated and subjected to size exclusion chromatography (Superdex™200 Increase 10/300, GE Healthcare) in 25 mM Tris−HCI (pH 7.4), 150 mM NaCI, 0.5 mM TCEP (buffer B).

Untagged human  $\alpha$ -synuclein was expressed from the pET17b vector (Novagen) BL21 Escherichia coli cells and purified essentially as described.<sup>58</sup> Shortly, the expression of the protein was induced at 37 °C for 3 hours. cells pelleted and periplasm proteins released by incubation in the osmotic shock buffer (40% v/v sucrose in 30 mM Tris HCl pH 7.2, 2 mM EDTA) at room temperature for 10 min and subsequently in ice-cold 2 mM MgCl2 for 3 min. Periplasmic extract was loaded on the strong anionexchange column HiPrep Q FF (GE Healthcare) and bound synuclein was eluted by running a 0-500 mM NaCl gradient. Synuclein-containing fractions were pooled, concentrated using 3 kDa cutoff-filters (Vivaspin 15R, Sartorius) and loaded on the gel filtration column HiLoad Superdex 200 16/600 (GE Healthcare). The relevant fractions were concentrated using Vivaspin 15R, heated at 95 °C for 30 min and precipitates separated by centrifugation. The remaining supernatant was gel-filtrated again. Synuclein concentration was determined at 280 nm applying a molar extinction coefficient of 5960 M<sup>-1</sup> cm<sup>-1</sup>.

# Isolation of synaptic vesicles from rat brains

Synaptic vesicles (SVs) were isolated according to previous publications. <sup>59,60,38</sup> Briefly, 20 rat brains were homogenized in ice-cold sucrose buffer (320 mM sucrose, 4 mM HEPES-KOH, pH 7.4 supplemented with 0.2 mM phenylmethylsulfonylfluoride and 1 mg/ml pepstatin A). Cellular debris was removed by centrifugation (10 min at  $900g_{Av}$ , 4  $^{\circ}$ C) and the resulting supernatant was further centrifuged for 10 min at 12,000 g<sub>Av</sub>, 4 °C. The pellet containing synaptosome was washed once by carefully resuspending it in sucrose buffer and further centrifuged for 15 min at 14,500 g<sub>Av</sub>, 4 °C. Synaptosomes were lysed by hypo-osmotic shock and free, released SVs were obtained after centrifugation of the lysate for 20 min at 14,500 g<sub>Av</sub>, 4 °C. The supernatant containing the SVs was further ultracentrifuged for 2 h, yielding a crude synaptic vesicle pellet. SVs were purified by resuspending the pellet in 40 mM sucrose followed by centrifugation for 3 h at 110,880 $g_{Av}$  on a continuous sucrose density gradient (50-800 mM sucrose). SVs were collected from the gradient and subjected to size-exclusion

chromatography on controlled pore glass beads (300 nm diameter), equilibrated in glycine buffer (300 mM glycine, 5 mM HEPES, pH 7.40, adjusted using KOH), to separate synaptic vesicles from residual larger membrane contaminants. SVs were pelleted by centrifugation for 2 hr at 230,000  $g_{\rm Av}$  and resuspended in sucrose buffer by homogenization before being aliquoted into single-use fractions and snap frozen in liquid  $N_2$ . The molar concentration of SVs was determined by measuring the total protein concentration where  $\sim\!100$  ng/ $\mu$ L of total SV protein corresponds to  $\sim\!10$  nM of SVs, according to previously established quantitative relationship.  $^{37}$ 

Western blot of contaminants and synaptic vesicle proteins. Proteins were transferred from a Tris-Glycine SDS-PAGE gel onto Amersham Hybond LFP membrane (0.2 µm, Cytiva). Wet transfer was done after standard protocol for either 1.5 h at 80 V at room temperature or overnight at 10 V at 4 °C. For washing and blocking steps TBS was used. Blocking was performed for 1 h at room temperature, while the blocking agent (3% BSA or 5% MLK in TBS) depended upon the primary antibody combination. Incubation with primary antibody was typically performed overnight with shaking: (Synaptophysin 1 [1:4000 in 3% BSA/ TBS, Sysy 101 011], Synaptobrevin 2 [1:8000 in 3% BSA/TBS, Sysy 104 211], NSF [1:5000 in 3% BSA/TBS, Sysy 123 011], Synaptotagmin [1:1000 in 5% MLK/TBS, Sysy 105 011], PSD95 [1:1000 in 5% MLK/TBS, Sysy 124 011], SDHA [1:1000 in 5% MLK/TBS, Abcam ab14715], Na<sup>+</sup>/K<sup>+</sup>-ATPase [1:1000 in 5%MLK/TBS, Merck/Millipore 05-369]). For fluorescent detection Cv3-conjugated (goat-α-mouse-IgG-Cy3) secondary antibodies from the Amersham ECL Plex™Detection kit were used according to manufacturer's instructions (1:2500 in 5%MLK/TBS, Cytiva). Fluorescence detection was performed using a Typhoon Trio Variable Imager System (GE Healthcare) by Cy3 excitation with the green laser (532 nm) and Cy3 emission filter settings (580 nm BP 30 nm).

# **Preparation of liposomes**

In this study, we used 1,2-dioleoyl-sn-glycero-3-phosphocholine (DOPC) from Avanti Polar Lipids. To prepare small unilamellar liposomes, DOPC was mixed and dissolved in chloroform (total concentration of 5 mM), dried first under a mild stream of N2 and then in desiccator overnight. Dried lipid films were rehydrated in 25 mM Tris—HCI (pH 7.4), 150 mM NaCI, 0.5 mM TCEP. Liposomes were formed by ten freeze (liquid N2) – thaw (37 °C water bath) cycles. Finally, the liposomes were extruded 21 times through the 50 nm-diameter polycarbonate filters (Avanti Polar Lipids).

# In vitro reconstitution of synapsin-SV condensates and data analysis

Optical density at 405 nm was measured every 10 minutes for at least 45 hours at 37  $^{\circ}\text{C}$  by using a Synergy H1 Hybrid Multi-Mode Microplate Reader (BioTek Instruments). A 30  $\mu\text{L}$  reaction mixture was set up at 4  $^{\circ}\text{C}$ , transferred to a 384-well microtiter plate (Greiner Bio-One, #781906) and preincubated for 5 minutes at 37  $^{\circ}\text{C}$  prior measurement. All the measurements were done in the following buffer: 25 mM Tris–HCl (pH 7.4), 150 mM NaCl, 0.5 mM TCEP.

For protein-only measurements, the raw data is plotted for each condition. In SV titration experiments 3  $\mu$ M synapsin 1 and 1  $\mu$ M  $\alpha$ -synuclein were incubated with SVs at the following final concentrations: 70 nM, 35 nM 23 nM 11.5 nM 5.9 nM.

For examining the effect of increasing concentration of  $\alpha$ -synuclein, the final protein concentration was fixed at 8 µM in which synapsin 1 and  $\alpha$ -synuclein were mixed at 3:1, 1:1 or 1:3 molar ratios, as indicated in the text. Synaptic vesicles were added at 23 nM, following the average physiological molar ratio of synapsin to 3,38 The condition where the molar ratio of synapsin 1, α-synuclein and SVs mimicked the physiological (6 μM, 2 μM and 23 nM, respectively) was used as a reference for normalizing the remaining curves in Figure 6(a). Three independent measurements (each containing a unique isolation of SVs) were done for each sample; all the data are represented as a mean ± standard error of the mean.

For examining the kinetic effect of  $\alpha$ -synuclein's presence during condensate formation the concentrations of synapsin 1 (2  $\mu$ M) and SVs (23 nM) were fixed.  $\alpha$ -Synuclein was added to a final concentration of 0.67  $\mu$ M or 6  $\mu$ M to reach a synapsin 1 to  $\alpha$ -synuclein ratio to 3:1 and 1:3, respectively. Three independent measurements were done for each sample; all the data are represented as a mean  $\pm$  standard deviation.

#### Thioflavin T aggregation assay

Fluorescence (excitation at 440 nm, emission at 484 nm) was measured every 20 minutes for 50 hours at 37 °C, double orbital shaking (425 cpm, 3 mm) for 5 s prior to recording, by using a Synergy H1 Hybrid Multi-Mode Microplate Reader (BioTek Instruments). A 30  $\mu$ L reaction mixture was set up at 4 °C, transferred to a 384-well microtiter plate (Greiner Bio-One, #781906). All the measurements were done in the following buffer: 25 mM Tris–HCl (pH 7.4), 150 mM NaCl, 0.5 mM TCEP. Thioflavin T (T3516, Sigma Aldrich) was added to a final concentration of 50  $\mu$ M. As a positive control for fibrillation, we used 46  $\mu$ M amyloid- $\beta$  (AS-72216, AnaSpec). As the negative controls, we used 46  $\mu$ M amyloid- $\beta$ 

mixed with the accompanying inhibitor (AS-72214, AnaSpec) and 46  $\mu$ M BSA.

# CRediT authorship contribution statement

Christian **Hoffmann:** Conceptualization, Methodology, Investigation, Validation, Writing original draft, Writing - review & editing. Roberto Conceptualization, Methodology, Sansevrino: Investigation, Validation, Writing - original draft, Writing - review & editing. Giuseppe Morabito: Methodology, Validation, Writing - review & editina. Chinyere Logan: Methodology, Validation, Writing - review & editing, R. Martin Vabulas: Methodology, Writing - review & editing. Ayse Ulusoy: Methodology, Writing - review & Ganzella: Methodology, editing. Marcelo Investigation, Validation, Writing - review & Dragomir Milovanovic: editing. Conceptualization, Methodology, Writing - original draft, Writing - review & editing, Supervision, Project administration, Funding acquisition.

# **Acknowledgements**

We are indebted to Dr. Reinhard Jahn (Max Planck Institute for Biophysical Chemistry, Germany) for the generous support to use the resources needed for the preparation of native vesicles, especially under these synaptic complicated circumstances. We thank the Advanced BioMedical Imaging facility at Charité for the support in microscopy; to Florian Aust, Franziska Trnka and Han Wang (all DZNE, Germany) for experimental support. D.M. is supported by the basic funds of DZNE and the CRC 1286 of the German Research Foundation.

# **Author contribution**

C.H., R.S. and D.M. designed the experiments. C. H., R.S., G.M., C.L., R.M.V., A.U., M.G. and D.M. performed the experiments. C.H., R.S. and D.M. wrote the paper. All authors read and approved the final manuscript.

# **Declaration of interests**

The authors declare no competing interests.

# Appendix A. Supplementary material

Supplementary data to this article can be found online at https://doi.org/10.1016/j.jmb.2021. 166961.

Received 19 November 2020; Accepted 19 March 2021; Available online 25 March 2021

#### Keywords:

liquid-liquid phase separation; synaptic vesicles; synapsin 1; α-synuclein; synucleinopathies

† These authors contributed equally.

## References

- Fernández-Busnadiego, R., Zuber, B., Maurer, U.E., Cyrklaff, M., Baumeister, W., Lucic, V., (2010). Quantitative analysis of the native presynaptic cytomatrix by cryoelectron tomography. *J. Cell Biol.*, 188, 145–156.
- Rizzoli, S.O., Betz, W.J., (2004). The structural organization of the readily releasable pool of synaptic vesicles. *Science*, 303, 2037–2039.
- Joensuu, M., Padmanabhan, P., Durisic, N., Bademosi, A. T.D., Cooper-Williams, E., Morrow, I.C., Harper, C.B., Jung, W., et al., (2016). Subdiffractional tracking of internalized molecules reveals heterogeneous motion states of synaptic vesicles. *J. Cell Biol.*, 215, 277–292.
- Milovanovic, D., De Camilli, P., (2017). Synaptic vesicle vlusters at synapses: A distinct liquid phase?. *Neuron*, 93, 995–1002.
- Wu, Y., Whiteus, C., Xu, C.S., Hayworth, K.J., Weinberg, R.J., Hess, H.F., De Camilli, P., (2017). Contacts between the endoplasmic reticulum and other membranes in neurons. *Proc. National Acad. Sci.*, 114, E4859–E4867.
- Wu, Y., O'Toole, E.T., Girard, M., Ritter, B., Messa, M., Liu, X., McPherson, P.S., Ferguson, S.M., et al., (2014). A dynamin 1-, dynamin 3- and clathrin-independent pathway of synaptic vesicle recycling mediated by bulk endocytosis. *Elife*, 3, e01621.
- De Camilli, P., Benfenati, F., Valtorta, F., Greengard, P., (1990). The synapsins. Annu. Rev. Cell Dev. Biol., 6, 433– 460.
- 8. Südhof, T.C., Czernik, A.J., Kao, H.T., Takei, K., Johnston, P.A., Horiuchi, A., Kanazir, S.D., Wagner, M.A., et al., (1989). Synapsins: mosaics of shared and individual domains in a family of synaptic vesicle phosphoproteins. *Science*, **245**, 1474–1480.
- Milovanovic, D., Wu, Y., Bian, X., De Camilli, P., (2018). A liquid phase of synapsin and lipid vesicles. *Science*, 361, 604–607.
- Chi, P., Greengard, P., Ryan, T.A., (2001). Synapsin dispersion and reclustering during synaptic activity. *Nature Neurosci.*, 4, 1187–1193.
- Clayton, D.F., George, J.M., (1998). The synucleins: a family of proteins involved in synaptic function, plasticity, neurodegeneration and disease. *Trends Neurosci.*, 21, 249–254.
- Burré, J., Sharma, M., Südhof, T.C., (2018). Cell biology and pathophysiology of α-synuclein. CSH Perspect. Med., 8, a024091.
- Wilhelm, B.G., Mandad, S., Truckenbrodt, S., Kröhnert, K., Schäfer, C., Rammner, B., Koo, S.J., Claßen, G.A., et al., (2014). Composition of isolated synaptic boutons reveals

- the amounts of vesicle trafficking proteins. *Science*, **344**, 1023–1028.
- 14. Fauvet, B., Fares, M.-B., Samuel, F., Dikiy, I., Tandon, A., Eliezer, D., Lashuel, H.A., (2012). Characterization of semisynthetic and naturally Nα-acetylated α-synuclein in vitro and in intact cells. *J. Biol. Chem.*, 287, 28243–28262.
- Burré, J., Vivona, S., Diao, J., Sharma, M., Brunger, A.T., Südhof, T.C., (2013). Properties of native brain αsynuclein. *Nature*, 498 E4 6-discussion E6–7.
- Theillet, F.-X., Binolfi, A., Bekei, B., Martorana, A., Rose, H.M., Stuiver, M., Verzini, S., Lorenz, D., et al., (2016). Structural disorder of monomeric α-synuclein persists in mammalian cells. *Nature*, **530**, 45–50.
- Bartels, T., Choi, J.G., Selkoe, D.J., (2011). α-Synuclein occurs physiologically as a helically folded tetramer that resists aggregation. *Nature*, 477, 107–110.
- 18. Nuber, S., Rajsombath, M., Minakaki, G., Winkler, J., Müller, C.P., Ericsson, M., Caldarone, B., Dettmer, U., et al., (2018). Abrogating native α-synuclein tetramers in mice causes a L-DOPA-responsive motor syndrome closely resembling Parkinson's Disease. *Neuron*, 100 75–90.e5.
- Jo, E., McLaurin, J., Yip, C.M., George-Hyslop, P.S., Fraser, P.E., (2000). alpha-Synuclein membrane interactions and lipid specificity. *J. Biol. Chem.*, 275, 34328–34334.
- Burré, J., Sharma, M., Südhof, T.C., (2014). α-Synuclein assembles into higher-order multimers upon membrane binding to promote SNARE complex formation. *Proc. National Acad. Sci.*, 111, E4274–E4283.
- Burré, J., Sharma, M., Tsetsenis, T., Buchman, V., Etherton, M.R., Südhof, T.C., (2010). Alpha-synuclein promotes SNARE-complex assembly in vivo and in vitro. *Science*, 329, 1663–1667.
- 22. Greten-Harrison, B., Polydoro, M., Morimoto-Tomita, M., Diao, L., Williams, A.M., Nie, E.H., Makani, S., Tian, N., et al., (2010). αβγ-Synuclein triple knockout mice reveal age-dependent neuronal dysfunction. *Proc. National Acad. Sci..* 107, 19573–19578.
- Vargas, K.J., Makani, S., Davis, T., Westphal, C.H., Castillo, P.E., Chandra, S.S., (2014). Synucleins regulate the kinetics of synaptic vesicle endocytosis. *J. Neurosci.*, 34, 9364–9376.
- Busch, D.J., Oliphint, P.A., Walsh, R.B., Banks, S.M.L., Woods, W.S., George, J.M., Morgan, J.R., (2014). Acute increase of α-synuclein inhibits synaptic vesicle recycling evoked during intense stimulation. *Mol. Biol. Cell*, 25, 3926–3941.
- Atias, M., Tevet, Y., Sun, J., Stavsky, A., Tal, S., Kahn, J., Roy, S., Gitler, D., (2019). Synapsins regulate α-synuclein functions. *Proc. National Acad. Sci.*, 116, 11116–11118.
- Gitler, D., Takagishi, Y., Feng, J., Ren, Y., Rodriguiz, R.M., Wetsel, W.C., Greengard, P., Augustine, G.J., (2004). Different presynaptic roles of synapsins at excitatory and inhibitory synapses. *J. Neurosci.*, 24, 11368–11380.
- Rosahl, T.W., Spillane, D., Missler, M., Herz, J., Selig, D. K., Wolff, J.R., Hammer, R.E., Malenka, R.C., et al., (1995). Essential functions of synapsins I and II in synaptic vesicle regulation. *Nature*, 375, 488–493.
- 28. Vargas, K.J., Schrod, N., Davis, T., Fernández-Busnadiego, R., Taguchi, Y.V., Laugks, U., Lucic, V., Chandra, S.S., (2017). Synucleins have multiple effects on presynaptic architecture. *Cell Rep.*, 18, 161–173.

- Woods, W.S., Boettcher, J.M., Zhou, D.H., Kloepper, K.D., Hartman, K.L., Ladror, D.T., Qi, Z., Rienstra, C.M., et al., (2007). Conformation-specific binding of alpha-synuclein to novel protein partners detected by phage display and NMR spectroscopy. J. Biol. Chem., 282, 34555–34567.
- Perego, E., Reshetniak, S., Lorenz, C., Hoffmann, C., Milovanović, D., Rizzoli, S.O., Köster, S., (2020). A minimalist model to measure interactions between proteins and synaptic vesicles. Sci. Rep., 10, 21086.
- Benfenati, F., Valtorta, F., Chieregatti, E., Greengard, P., (1992). Interaction of free and synaptic vesicle-bound synapsin I with F-actin. *Neuron*, 8, 377–386.
- Schmidt, H.B., Görlich, D., (2015). Nup98 FG domains from diverse species spontaneously phase-separate into particles with nuclear pore-like permselectivity. *Elife*, 4, e04251.
- Lin, Y., Mori, E., Kato, M., Xiang, S., Wu, L., Kwon, I., McKnight, S.L., (2016). Toxic PR poly-dipeptides encoded by the C9orf72 repeat expansion target LC domain polymers. *Cell*, 167, 789–802.e12.
- 34. Shupliakov, O., (2009). The synaptic vesicle cluster: a source of endocytic proteins during neurotransmitter release. *Neuroscience*, **158**, 204–210.
- Denker, A., Kröhnert, K., Bückers, J., Neher, E., Rizzoli, S. O., (2011). The reserve pool of synaptic vesicles acts as a buffer for proteins involved in synaptic vesicle recycling. *Proc. National Acad. Sci.*, 108, 17183–17188.
- Reshetniak, S., Ußling, J., Perego, E., Rammner, B., Schikorski, T., Fornasiero, E.F., Truckenbrodt, S., Köster, S., et al., (2020). A comparative analysis of the mobility of 45 proteins in the synaptic bouton. *EMBO J.*, 39, e104596.
- Medeiros, A.T., Soll, L.G., Tessari, I., Bubacco, L., Morgan, J.R., (2017). α-Synuclein dimers impair vesicle fission during clathrin-mediated synaptic vesicle recycling. Front. Cell. Neurosci., 11, 388.
- Takamori, S., Holt, M., Stenius, K., Lemke, E.A., Grønborg, M., Riedel, D., Urlaub, H., Schenck, S., et al., (2006). Molecular anatomy of a trafficking organelle. *Cell*, 127, 831–846.
- Georgieva, E.R., Ramlall, T.F., Borbat, P.P., Freed, J.H., Eliezer, D., (2008). Membrane-bound α-synuclein forms an extended helix: long-distance pulsed ESR measurements using vesicles, bicelles, and rodlike micelles. *J. Am. Chem.* Soc., 130, 12856–12857.
- 40. Bodner, C.R., Dobson, C.M., Bax, A., (2009). Multiple tight phospholipid-binding modes of α-synuclein revealed by solution NMR spectroscopy. *J. Mol. Biol.*, 390, 775–790.
- Middleton, E.R., Rhoades, E., (2010). Effects of curvature and composition on α-synuclein binding to lipid vesicles. *Biophys. J.*, 99, 2279–2288.
- Diao, J., Burré, J., Vivona, S., Cipriano, D.J., Sharma, M., Kyoung, M., Südhof, T.C., Brunger, A.T., (2013). Native αsynuclein induces clustering of synaptic-vesicle mimics via binding to phospholipids and synaptobrevin-2/VAMP2. *Elife*, 2, e00592.
- 43. Lautenschläger, J., Stephens, A.D., Fusco, G., Ströhl, F., Curry, N., Zacharopoulou, M., Michel, C.H., Laine, R., et al., (2018). C-terminal calcium binding of α-synuclein modulates synaptic vesicle interaction. *Nature Commun.*, 9, 712.
- Wang, L., Das, U., Scott, D.A., Tang, Y., McLean, P.J., Roy, S., (2014). α-Synuclein multimers cluster synaptic vesicles and attenuate recycling. *Curr. Biol.*, 24, 2319– 2326.

- Pieribone, V.A., Shupliakov, O., Brodin, L., Hilfiker-Rothenfluh, S., Czernik, A.J., Greengard, P., (1995).
  Distinct pools of synaptic vesicles in neurotransmitter release. *Nature*, 375, 493–497.
- Villar-Piqué, A., da Fonseca, T.L., Outeiro, T.F., (2016).
  Structure, function and toxicity of alpha-synuclein: the Bermuda triangle in synucleinopathies. *J. Neurochem.*, 139, 240–255.
- 47. Kramer, M.L., Schulz-Schaeffer, W.J., (2007). Presynaptic α-synuclein aggregates, not Lewy bodies, cause neurodegeneration in dementia with Lewy bodies. *J. Neurosci.*, 27, 1405–1410.
- 48. Nemani, V.M., Lu, W., Berge, V., Nakamura, K., Onoa, B., Lee, M.K., Chaudhry, F.A., Nicoll, R.A., et al., (2010). Increased expression of α-synuclein reduces neurotransmitter release by inhibiting synaptic vesicle reclustering after endocytosis. *Neuron*, 65, 66–79.
- Li, P., Banjade, S., Cheng, H.-C., Kim, S., Chen, B., Guo, L., Llaguno, M., Hollingsworth, J.V., et al., (2012). Phase transitions in the assembly of multivalent signalling proteins. *Nature*, 483, 336–340.
- Sun, J., Wang, L., Bao, H., Premi, S., Das, U., Chapman, E.R., Roy, S., (2019). Functional cooperation of αsynuclein and VAMP2 in synaptic vesicle recycling. *Proc. National Acad. Sci.*, 116, 11113–11115.
- Stöckl, M., Fischer, P., Wanker, E., Herrmann, A., (2008).
  α-Synuclein selectively binds to anionic phospholipids embedded in liquid-disordered domains. *J. Mol. Biol.*, 375, 1394–1404.
- van Rooijen, B.D., Claessens, M.M.A.E., Subramaniam, V., (2008). Membrane binding of oligomeric α-synuclein depends on bilayer charge and packing. *FEBS Lett.*, **582**, 3788–3792.
- 53. Patel, A., Lee, H.O., Jawerth, L., Maharana, S., Jahnel, M., Hein, M.Y., Stoynov, S., Mahamid, J., et al., (2015). A liquid-to-solid phase transition of the ALS protein FUS accelerated by disease mutation. *Cell*, 162, 1066–1077.
- Shin, Y., Brangwynne, C.P., (2017). Liquid phase condensation in cell physiology and disease. *Science*, 357, eaaf4382.
- 55. Ray, S., Singh, N., Kumar, R., Patel, K., Pandey, S., Datta, D., Mahato, J., Panigrahi, R., et al., (2020). α-Synuclein aggregation nucleates through liquid–liquid phase separation. *Nature Chem.*, 12, 705–716.
- Wang, X., Becker, K., Levine, N., Zhang, M., Lieberman, A. P., Moore, D.J., Ma, J., (2019). Pathogenic alpha-synuclein aggregates preferentially bind to mitochondria and affect cellular respiration. *Acta Neuropathol. Commun.*, 7, 41.
- 57. Shahmoradian, S.H., Lewis, A.J., Genoud, C., Hench, J., Moors, T.E., Navarro, P.P., Castaño-Díez, D., Schweighauser, G., et al., (2019). Lewy pathology in Parkinson's disease consists of crowded organelles and lipid membranes. *Nature Neurosci.*, 22, 1099–1109.
- 58. Huang, C., Ren, G., Zhou, H., Wang, C., (2005). A new method for purification of recombinant human α-synuclein in Escherichia coli. *Protein Expres. Purif.*, 42, 173–177.
- Nagy, A., Baker, R.R., Morris, S.J., Whittaker, V.P., (1976).
  The preparation and characterization of synaptic vesicles of high purity. *Brain Res.*, 109, 285–309.
- Huttner, W.B., Schiebler, W., Greengard, P., De Camilli, P., (1983). Synapsin I (protein I), a nerve terminal-specific phosphoprotein. III. Its association with synaptic vesicles studied in a highly purified synaptic vesicle preparation. *J. Cell Biol.*, 96, 1374–1388.